International Journal of Nanomedicine

Dovepress
open access to scientific and medical research

Open Access Full Text Article

ORIGINAL RESEARCH

Nanoparticle Encapsulation of the Hexane Fraction of *Cyperus Rotundus* Extract for Enhanced Antioxidant and Anti-Inflammatory Activities in vitro

Chaehyun Kim[1,2], Sangwoo Kim[1,3], Ah-Reum Jung[4], Jun-Hwan Jang[4,5], Juntae Bae[4], Won Il Choi[1], Daekyung Sung[1]

[1]Center for Bio-Healthcare Materials, Bio-Convergence Materials R&D Division, Korea Institute of Ceramic Engineering and Technology, Cheongju, 28160, Republic of Korea; [2]Department of Applied Bioengineering, Graduate School of Convergence Science and Technology, Seoul National University, Seoul, 08826, Republic of Korea; [3]Department of Chemical and Biomolecular Engineering, Yonsei University, Seoul, 03722, Republic of Korea; [4]J2K-Metabiome, J2KBIO, Cheongju, 28104, Republic of Korea; [5]College of Pharmacy, Chungbuk National University, Cheongju, Republic of Korea

Correspondence: Daekyung Sung, Center for Bio-Healthcare Materials, Bio-Convergence Materials R&D Division, Korea Institute of Ceramic Engineering and Technology, Cheongju, 28160, Republic of Korea, Tel +82-43-913-1511, Fax +82-43-913-1597, Email dksung@kicet.re.kr

Aim: *Cyperus rotundus* L. (CR) is traditionally used in medicine for its anti-inflammatory properties. In particular, α-cyperone, which is isolated from the essential oil and found primarily in the n-hexane fraction of the ethanolic extract, is known to inhibit NO production in LPS-stimulated RAW 264.7 cells. However, high concentrations of α-cyperone are required for sufficient anti-inflammatory activity. Even, essential oil obtained from *C. rotundus* has the disadvantage of low solubility and stability in aqueous environment, which makes it difficult to be applied in various fields and easily loses its activity. Therefore, in this study, we aimed to increase the extraction yield of *C. rotundus* by microbubble extraction and prepare nanoparticles (NPs) that can preserve its activity in a stable and bioavailable manner by utilizing nanoprecipitation.

Methods: *C. rotundus* rhizomes were extracted in 50% ethanol using microbubbles and then fractionated with n-hexane to obtain α-cyperone-rich *C. rotundus* n-hexane fraction (CRHF). The biodegradable plant extract, α-cyperone, was prepared as green nanoparticles (CR@NPs) by nanoprecipitation technique under mild reaction conditions. The physicochemical properties of CR@NPs, including size, polydispersity index, and surface charge, were determined using dynamic light scattering. The extraction yield and encapsulation efficiency of α-cyperone were quantified by high-performance liquid chromatography. Antioxidant and anti-inflammatory activities were evaluated by DPPH assay and in vitro ROS and NO assays, and biocompatibility was assessed by MTT assay.

Results: *C. rotundus* loaded nanoparticles demonstrated overcoming the limitation of α-cyperone solubility and stability in CRHF and also the antioxidant, anti-inflammatory properties as evidenced by in vitro assays in cellular models.

Conclusion: The versatility of green chemistry, such as α-cyperone, enables the production of nanoparticles with promising biomedical applications such as cosmetics, pharmaceuticals, and food products.

Keywords: α-cyperone, solubilization, nanoparticle, encapsulation, nanoprecipitation, SJC-clearsol D

Introduction

Cyperus rotundus L., commonly known as purple nutsedge or nutgrass, is a well-known traditional medicinal plant in the Cyperaceae family.[1] It is found in tropical, subtropical, and temperate regions and is used in traditional Indian, Chinese, and Japanese medicine.[2] Several studies have highlighted the rhizomes of *C. rotundus L.* as an effective source of natural antioxidants and anti-inflammatory.[3–5] In particular, α-cyperone, one of the major components of *C. rotundus* essential oil,[6] is predominantly found in the n-hexane fraction of the plant, and its anti-inflammatory effect has been shown to be higher than that of whole ethanol extract;[7] however, high concentrations of α-cyperone are required to show an inhibitory effect on LPS-induced NO production in RAW 264.7 cells.[7,8] We attempted to enhance the anti-inflammatory effect of

Received: 18 December 2023
Accepted: 12 July 2024
Published: 16 August 2024

CRHF, containing α-Cyperone, in LPS stimulated RAW 264.7 cells by extracting more essential oils of *C. rotundus* with microbubble generator.[9] Micro-bubbles can be used to extract organic compounds, such as α-cyperone, from water solutions.[10] Bredwell and Worden[11] reported that microbubbles enable a higher mass transfer rate with lower power consumption and that the mass transfer coefficient for a microbubble system is significantly higher than that of conventional bubbles. Therefore, the microbubble generator enabled the extraction of more *C. rotundus* from ethanol and subsequently provided increased amounts of essential oils, mainly found in the n-hexane fraction. However, the α-cyperone mainly found in CRHF essential oils is fat-soluble, meaning it loses its activity when used in an aqueous environment. The active ingredient is rapidly released into the environment after application and gradually degraded, resulting in low persistence.[12,13] To overcome these drawbacks, encapsulation of CRHF into nanoparticles could be an effective strategy for their use as drug delivery carriers in biomedical applications.[14] The encapsulation process provides many benefits and opens up wide range of possible applications, including protecting sensitive active compounds and shielding them from external influences, such as moisture, oxygen, heat, and light,[15] or to delivering them to specific sites to ensure localized drug delivery while minimizing side effects.[16] Various physical, chemical, and biological methods are used to synthesize nanoparticles. Many of these methods, particularly physical and chemical methods, rely on the use of potentially harmful stabilizers or non-biodegradable reagents.[17] On the contrary, employing biological materials such as plant extracts to produce nanoparticles enables quick and economical "green synthesis" methods that forego toxic solvents and do not pollute the environment.[18,19] Therefore, various studies have utilized *C. rotundus* rhizomes to create green nanomaterials. However, many earlier studies required intricate techniques or high temperatures for synthesis,[20,21] making it difficult to preserve the natural medicinal properties of *C. rotundus*, particularly its anti-inflammatory effects.

In this study, *C. rotundus* was processed into nanoparticles using nanoprecipitation combined with solubilizers to augment its stability and enhance its loading capacity with the aim of improving its anti-inflammatory and antioxidant properties.[22]

Nanoprecipitation is an intriguing approach to rapidly produce green nanoparticles that encapsulate essential oils from *C. rotundus*, and have low sensitivity to minor variations.[14] Additionally, green chemistry is energy-efficient, which allows for effective scaling up to an industrial level.[23] This effective technique generates precisely formed polymeric colloids that can be used as carriers in various biomedical applications.[24] This encompasses a range of applications, including chemotherapy to treat disease and local cosmetic treatments to improve aesthetic outcomes.[13,25]

Materials and Methods

The *Cyperus rotundus Linn. (Linnaeus.)*, formally identified by the botanist Linnaeus, used in this experiment was purchased from SamHonggeonjaeyakeop, a traditional medicinal ingredient store located in Namyangju-si, Gyeonggi-do, Republic of Korea. This plant was harvested in Goryeong-gun, Gyeongsangbuk-do, in 2022. Botanical identification was formally carried out from the Bio-Convergence Materials R&D Division, Korea Institute of Ceramic Engineering and Technology, according to the classification list of Cyperaceae in the Korean Peninsula by the Korea National Arboretum (2014). A voucher specimen (CR-2302) has been deposited in the Smart Nano Convergence Materials Laboratory at the Bio-Convergence Materials R&D Division, Korea Institute of Ceramic Engineering and Technology.

A hybrid microbubble generator (O2B-750S, O2Bubble Co., Ltd., Korea) was used for microbubble extraction. High-performance liquid chromatography (HPLC) was performed using the Alliance Waters e2695 system (Waters, Milford, MA, USA). A Capcell PAK C18 column (Osaka Soda Co.) was used. To analyze the main component, the standard substance α-cyperone was purchased from Sigma-Aldrich (USA). Deionized water (DIW) was purchased from HyClone (Logan, UT, USA) and SJC-Clearsol D from CU Chemical Co., Gyeonggi-do, South Korea. For methylene-blue staining analysis, methylene blue was purchased from Sigma-Aldrich, headquartered in St. Louis, Missouri, USA. For the in situ antioxidant experiments, ascorbic acid (AA) and 2, 2-diphenyl-1-picrylhydrazyl (DPPH) were obtained from Sigma Aldrich (St. Louis, Missouri, USA).

High-performance liquid chromatography-grade reagents including water, acetonitrile, and acetic acid were obtained from Sigma-Aldrich (St. Louis, MO, USA, for high-performance liquid chromatography (HPLC). NIH/3T3 cells (ATCC CRL-1658, MD, USA) were cultured in Dulbecco's modified Eagle's medium (DMEM), penicillin-streptomycin, fetal bovine serum (FBS), and 0.25% trypsin procured from Gibco (Grand Island, NY, USA) for in vitro assays. The

substances used in in vitro experiments were hydrogen peroxide (H_2O_2, 30%) procured from Junsei Chemical Co. (Tokyo, Japan), followed by 3-(4,5-dimethylthiazol-2-yl)-2,5-diphenyltetraazolium bromide (MTT), and finally, 2,7-dichlorodihydrofluorescein diacetate (H_2DCFDA), both sourced from Invitrogen (Carlsbad, CA, USA). Dimethyl sulfoxide-d6 (DMSO-d_6, 99.8%) was provided by Sigma-Aldrich, and phosphate-buffered saline (PBS pH 7.4) was purchased from Hyclone (Logan, UT, USA). For the anti-inflammatory assay, LPS and Griess reagent were purchased from Sigma-Aldrich (St. Louis, MO, USA).

Extraction of C. Rotundus

The rhizomes of *C. rotundus* (1000 g) were dried, and extracted with 50% ethanol (10,000 g) in a ratio of 1:10 at 60°C by using a hybrid microbubble generator equipped with a pore size of 5 to 50 μm and a discharge rate of 1.0 to 1.2 tons per hr (liquid flow rate) for 3 hr. After microbubble extraction, the extract was filtered through a 5 μm filter. The filtrate was concentrated under reduced pressure using a rotary evaporator, followed by three successive fractions with equal volumes of n-hexane. After concentration, approximately 5 g of hexane fraction was obtained from *C. rotundus* (Figure 1, Jaeseop Lee et al 2023).[26]

HPLC Analysis to Quantify the Major Component, α-Cyperone

HPLC analysis was carried out to determine the content of the major component, α-cyperone. The samples were prepared by accurately measuring the weight of α-cyperone and the *C. rotundus* hexane fraction, which contains the main component. These samples were then dissolved in 50% (v/v) methanol and filtered through a 0.45 μm PVDF membrane filter before analysis. The analytical conditions used are listed in Table 1.[27]

Fabrication of CR@NPs

The CR@NPs were formed by the self-assembly of hydrophobic CR with amphiphilic SJC-Clearsol D in the aqueous phase. SJC-Clearsol D consists of a hydrophobic hydrocarbon chain and a hydrophilic carboxyl group. Initially, CR (1, 2, 4, or 6 mg) and SJC-Clearsol D (20 mg) were combined in a 4 mL vial with 1 mL of EtOH, resulting in dissolution. The

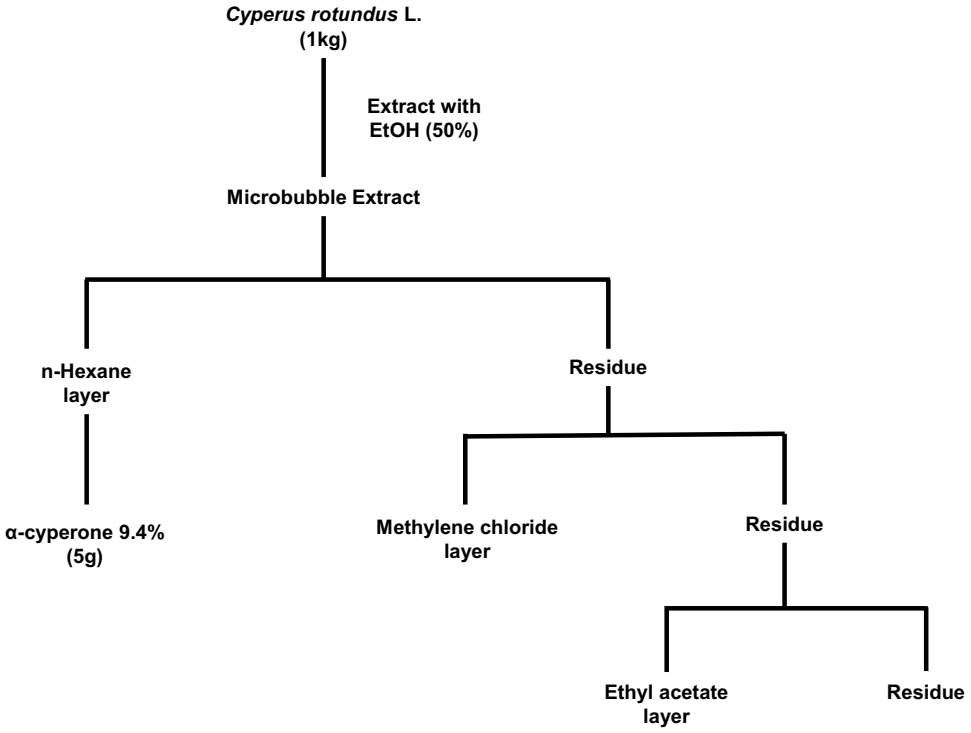

Figure 1 The extraction and fractionation process of *Cyperus rotundus*.

Table 1 Analytical Method for n-Hexane Fraction of Cyperus Rotundus by HPLC

HPLC	Waters e2695 / 2998 UVD			
Column	Capcellpak C_{18} UG 120 5 μm, 4.6×250 mm			
Solvent	A: 0.5% TFA in Water, B: MeOH			
Gradient condition	Time	Flow rate	A %	B %
	0	1.0 mL/min	50	50
	30 s	1.0 mL/min	20	80
	40 min	1.0 mL/min	10	0
	42 min	1.0 mL/min	0	100
	50 min	1.0 mL/min	0	100
	65 min	1.0 mL/min	50	50
	75 min	1.0 mL/min	50	50
Detection	UV 254 nm			
Temp	35 °C			
Injection volume	20 μL			

Note: Data from Seo et al.[27]

mixture was stirred by rotary shaker at room temperature for 2 h. Subsequently, CR containing EtOH solution was administered using a syringe pump (LEGATO100, KD Scientific, Korea) with stirring at 530 rpm, and SJC-Clearsol D was slowly added dropwise to 5 mL of deionized water.

The resulting CR@NPs (with CR loadings of 5, 10, 20, and 30 wt% relative to SJC-Clearsol D) were gently stirred at 530 rpm for 1 hr for stabilization. Finally, the solvent was thoroughly removed by vacuum evaporation over 2 hr period, and the remaining substance was diluted with deionized water (DIW) to achieve a final volume of 5 mL. The products obtained were named CR@NP × wt%, where × wt% represents the CR loading of SJC-Clearsol D. An identical procedure was followed to generate empty nanoparticles (NPs) from SJC-Clearsol D without the addition of CR, designated as 0 wt%.[28] The surface charge, particle diameter, and PDI of CR@NPs were assessed by DLS measurements using an electrophoretic light-scattering spectrophotometer (ELS-Z2; Otsuka Electronics Co., Tokyo, Japan). After purification of the unloaded CR using Amicon Ultra-15 centrifugal filters with a 100 kDa molecular weight cutoff, the loading efficiency and CR content in the nanoparticles were assessed using HPLC.

Ultrafiltration was performed at 1000 rpm for 3 min. The HPLC experiment utilized the following conditions: With a detection wavelength of 254 nm and a 20 μL injection volume, we used a mobile phase consisting of a water solution containing 1% acetic acid and acetonitrile. The eluent was consistently delivered at a rate of 1 mL/min. The study was carried out under conditions of 30 °C. The gradient program consisted of the following steps: from 0 to 25 min, there was a gradual increase from 50% to 80% B in A, from 25 to 35 min, there was a gradual increase from 80% to 100% B in A, and finally, from 35 to 40 min, there was an isocratic elution with 100% B. The loading content and efficiency are determined as:[1,29]

$$Loading\ content\ (\%) = \left[\frac{(weight\ of\ fed\ CR - weight\ of\ unloaded\ CR)}{weight\ of\ NPs}\right] \times 100$$

$$Loading\ efficiency\ (\%) = \left[\frac{(weight\ of\ fed\ CR - weight\ of\ unloaded\ CR)}{weight\ of\ fed\ CR}\right] \times 100$$

Measuring the Stability and Optical Clarity of CR@NPs

DLS was used to assess the stability of CR@NPs over 56 days. The size and PDI of CR@NPs were examined in DIW on days 1, 7, 14, 21, 28, and 56, covering a range of CR concentrations (0%, 5%, 10%, and 20% by weight).[30] To evaluate the clarity and stability of the encapsulation as well as the clarity of the distributed phase in the synthesized CR@NPs at various CR concentrations (0%, 5%, 10%, 20%, and 30% by weight), a dye dissolution procedure was applied using a hydrophilic dye, methylene blue. Initially, we prepared a methylene blue solution with a concentration of 6.25 μM by dissolving in deionized water (DIW). Subsequently, 2 mL of this dye solution was added into a 2 mL suspension containing CR@NPs, and the mixture was thoroughly mixed in a 4 mL vial. Finally, a visual inspection was conducted to determine whether the CR@NPs precipitated or dispersed in the solution.[31]

Assessment of the in situ Antioxidant Activity of CR@NPs Using DPPH Radical Scavenging Assays

The DPPH assay was used to assess the antioxidant activity of CR@NPs. Control groups were prepared using solutions with two concentrations (5 and 10 wt%) of AA and CR in DIW. In addition, CR@NPs were formulated with three different CR concentrations (0, 5, and 10 wt%). A 0.1 mM DPPH solution was diluted with ethanol and stirred for about 1 hr, and then kept in a dark environment at a temperature of 4 °C. Afterwards, each CR@NP suspension was combined with 150 μL of the prepared DPPH solution, resulting in a total volume of 200 μL. An untreated control group consisted of a 50 μL DPPH solution aliquot mixed with 150 μL DIW, which had minimal antioxidant activity. AA was used as a positive control, whereas CR in DIW and unloaded NP were used as negative controls for comparison with CR@NPs. The blends were incubated in the dark at 25 °C for 24 hr. The absorbance of each blend was measured at 515 nm using a microplate reader (VICTOR X5; Perkin Elmer). Antioxidant activity was assessed in the following manner:[32,33]

$$\textit{Antioxidant activity}\ (\%) = \frac{\Delta A_{515}\ \textit{of control} - \Delta A_{515}\ \textit{of sample}}{\Delta A_{515}\ \textit{of control}} \times 100$$

Assessment of in vitro Antioxidant Activity of CR@NPs Using H_2DCFDA Solution

To assess the cellular antioxidant effect of CR@NPs containing 10 wt% CR, NIH 3T3 mouse embryonic fibroblasts were cultured in 96-well plates at a seeding density of 10,000 cells per well and incubated for 24 hr. Reactive oxygen species (ROS) were induced in NIH 3T3 fibroblasts after exposure to H_2O_2, an oxidative stress agent. After treatment with the samples, the changes in ROS levels were evaluated using the following procedure: initially, fibroblast cells were exposed to mixtures of CR@NP 10 wt% with different CR concentrations (ranging from 10 ng/mL to 1μg/mL) and 10 μM hydrogen peroxide (H_2O_2), dissolved and cultured for 8 hr. A negative control group without H_2O_2 and a positive control group with H_2O_2 served as references. The NIH 3T3 cells were then rinsed with PBS (200 μL per 96-well plate) in order to eliminate any remaining sample solution, followed by treatment with a 10 μM H_2DCFDA solution (100 μL per 96-well plate) in the dark, serves as an indicator of ROS fluorescence. The cells were then incubated in the dark for 30 min. Finally, the in vitro antioxidant effectiveness of the samples was determined using a microplate reader to measure the fluorescence signal strength of dichlorofluorescein (DCF), which is oxidized by ROS, at an emission wavelength (535 nm) and an excitation wavelength of (485 nm).[29]

Assessment of in vitro Cytotoxicity of CR@NPs Using MTT Assay

The biocompatibility of the CR@NPs was evaluated using NIH 3T3 cells cultured in DMEM supplemented with 1% penicillin-streptomycin and 10% FBS. After the addition of CR@NPs, cell viability was examined after 24 hr using the 3-(4,5-dimethylthiazol-2-yl)-2,5-diphenyltetrazolium bromide (MTT) assay. Initially, cells were grown in 96-well plates, with each well containing 10,000 cells. Following a 24-hr incubation period, various concentrations of CR@NPs (1 to 100 μg/mL) were applied to the cells and cultured at 37 °C for 24 hr. Next, medium containing 1 mg/mL MTT solution was added, and each well of the plate was incubated with DMEM supplemented with 1% penicillin-streptomycin and 10% FBS for 3 hr. Finally, PBS was used to clean the medium, and DMSO-d_6 to dissolve the crystalline purple formazan dye.

The optical density of formazan produced by living cells was measured at 570 nm using a microplate reader (BioTek, Winooski, VT, USA). The percentage of viable cells was calculated using the following equation:[34]

$$Cell\ viability\ (\%) = \left(\frac{\Delta A_{570\ of\ test\ group}}{\Delta A_{570\ of\ control\ group}}\right) \times 100$$

Assessment of in vitro Anti-Inflammatory Activity of CR@NPs

To assess the anti-inflammatory properties of CR@NPs within the cell, RAW 264.7 cells were seeded in 96-well plates at a concentration of 15,000 cells per well (200 µL) and cultured for 24 hr. LPS induces an inflammatory response, leading to the generation of NO in RAW 264.7 cells. Changes in NO levels after application of the samples were assessed. Initially, RAW 264.7 cells were exposed to different concentrations (ranging from 0.01 to 10 µg/mL) of CR@NPs and LPS 20 ng/mL, and subsequently incubated for 24 hr. For comparison, a negative control without LPS was incubated in the absence of CR@NPs. After a 24-hr incubation period, the supernatant was transferred to a fresh 96-well plate and Griess reagent was added to each well. After introducing the Griess reagent into each well, the 96-well plates were incubated at room temperature for 10 min, and a microplate reader (VICTOR X5, PerkinElmer, Singapore, Republic of Singapore) was used to measure absorbance at a wavelength of 560 nm. NO production was determined by analyzing the in vitro anti-inflammatory activity of CR@NPs.[30,35]

Statistical Analysis

The experimental data were presented as mean ± standard deviation, and each experiment was performed in triplicate. To compare the variations between experimental groups, we used Student's *t*-test. Statistical significance was confirmed for all assessments with a p-value < 0.05.

Results and Discussion

Analysis of the Cyperus Rotundus Extract

CO_2 microbubbles, when used in conjunction with high-frequency sonic waves, are effective in disrupting cell walls due to their ability to cause repeated shrinking and expanding movements. This method utilizes carbon dioxide to form tiny bubbles that assist in breaking down the cell structures.[10,36] During the extraction of *C. rotundus* with a microbubble generator in ethanol, the extent to which it dissolves can be controlled by modifying the size and density of the bubbles.[37] As bubble sizes decrease to the micro-to-nanoscale, their increased surface area enhances the rate of dissolution, leading to a higher gas dissolution (mass transfer) rate.[38] We employed a microbubble generator to produce CO_2 microbubbles of 50 µm, which were then reduced to nanoscale using ultrasonic waves to facilitate the extraction of *C. rotundus*. HPLC analysis was performed to determine the content of α-cyperone in the hexane fraction of *C. rotundus*, and α-Cyperone (RT, 27.5 min) was identified and its content was 9.4%.

Characterization of CR@NPs

C. rotundus, commonly known as nutgrass, is a perennial sedge.[1] This plant is known for its natural hydrophobic bioactive compounds[39] which have diverse effects, including antioxidant and anti-inflammatory effects.[3,40] Nevertheless, the use of *C. rotundus L.* in the biological industry, particularly in pharmaceuticals, health foods, and skincare products, presents challenges because of its limited solubility and instability upon contact with water.[41] Therefore, in this study, SJC-Clearsol D NPs with diverse CR concentrations ranging from 0 to 30 wt% were formulated using an encapsulation method to address the need for a carrier that can improve the stability and solubility of lipophilic CR. SJC-Clearsol D self-organizes in water, resulting in the formation of stable nanoparticles. These nanoparticles possess a hydrophilic outer layer and a hydrophobic interior core, providing an environment suitable for encapsulating hydrophobic compounds (Figure 2A). No notable differences were observed in the physicochemical properties such as size and PDI of the CR@NPs when the CR concentration was varied from 0 to 30 wt%. (Figure 3A and B). In the case of unloaded NP (without CR), a slight zeta potential of −0.34 mV ± 0.49 was observed. At a CR@NP concentration of 10 wt%, the zeta potential value was −6.67 mV ± 2.93, which was very similar to the aforementioned value. As the CR concentration

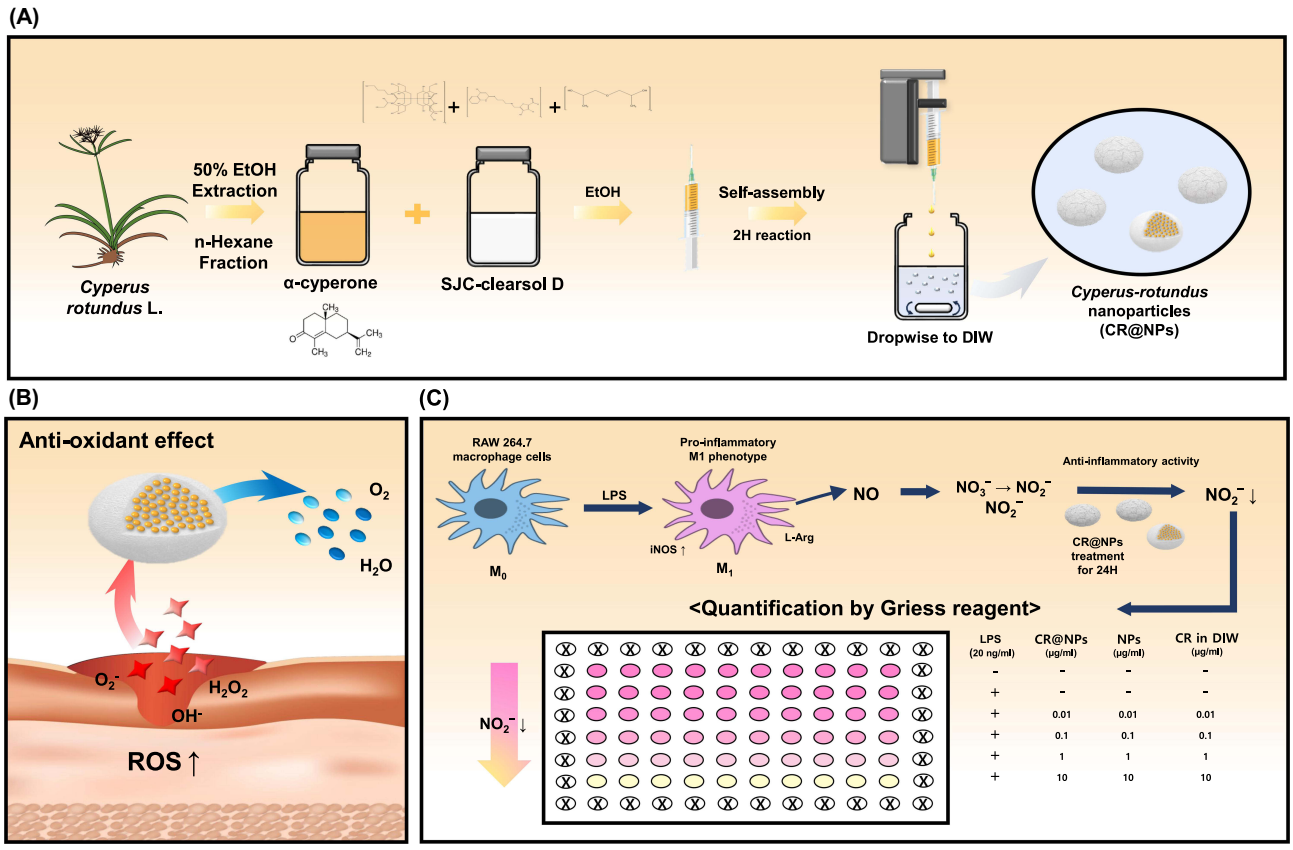

Figure 2 Schematic Diagram of (**A**) The fabrication process for CR@NPs, (**B**) Improved antioxidant effect of CR@NPs, and (**C**) Quantification of NO production and reduction through Griess reagent after treatment of LPS and CR@NPs for 24 hr in RAW264.7 macrophage cells.

increased to 30 wt%, the zeta potentials of the other CR@NPs tended to decrease progressively, resulting in more negative values. In particular, it was observed that the zeta potential further increased negatively to −24.36 mV ± 1.61 at a 30 wt% of CR concentration (Figure 3C). CR encapsulation within the CR@NPs was estimated by staining with the water-soluble dye, methylene blue. When CR dissolves in water, it is dispersed into fine particles and exhibits a cloudy appearance.

The more CR was incorporated into the CR@NPs, the more distinct and clear the particles became, whereas a lower loading rate resulted in hazier particle formation. Adding methylene blue resulted in transparent suspensions of CR@NPs containing CR concentrations up to 20 wt%, demonstrating the successful encapsulation of CR in the nanoparticles at this concentration threshold. However, when the CR concentration reached 30 wt.%, the suspensions became non-transparent, suggesting the existence of unencapsulated CR (Figure 3D). To measure the degree of CR encapsulation in CR@NPs, the CR loading content and efficiency were assessed using HPLC at various CR concentrations. The results are outlined below: For 5 wt% CR@NPs, the content loading (L.C.) was 4.6% with a loading efficiency (L.E.) of 92.05%. In the case of 10 wt% CR@NPs, L.C. was 9.81% and L.E. was 98.14%. Finally, for the 20 wt% CR@NPs, the L.C. was 17.37% and the L.E. was 86.87%.

Long-Term Stability of CR@NPs

Particles formed by the dispersion of oil in water are only temporarily stable because they have high energy; however, they are thermodynamically unstable Hence, oil-particle suspensions, are dispersed in water in the presence of surfactants, they are prone to phase separation owing to destabilization mechanisms such as aggregation, merging, and precipitation. Thus, the sustained stability of the CR@NPs was assessed under two conditions: (1) in an aqueous solution (DIW) at 25 °C and (2) after redispersion in DIW after cryodesiccation. First, the diameter (Figure 4A) and

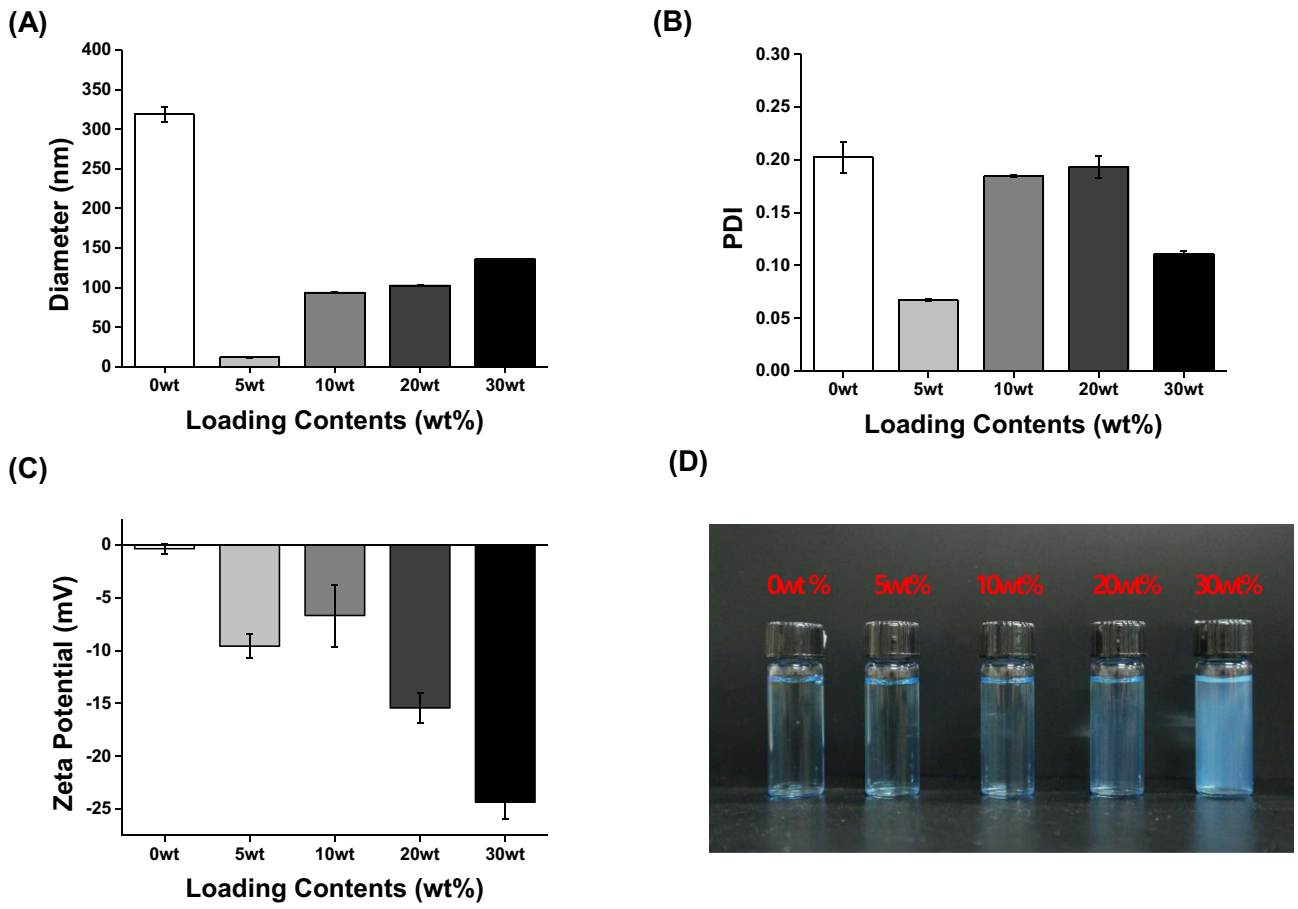

Figure 3 The initial stability of CR@NPs ranging from 0 wt% to 30wt% of CR: (**A**) Diameter of hydrodynamic particles, (**B**) Polydispersity index (PDI), (**C**) Zeta potential, and (**D**) Digital images after methylene-blue staining test.

PDI (Figure 4B) of CR@NPs in DIW remained stable without significant changes within the CR concentration range of 5–20 wt.% until 56 days. However, precipitation occurred for 20 wt% on the 56th day (Figure 4C), and CR@NPs at 20 wt % had lower loading efficiencies than the other initial particle concentrations. This explains why SJC-Clearsol D and CR, which did not form particles at 20 wt% CR@NPs, aggregated and precipitated over time. Secondly, CR@NPs with CR concentrations ranging from 0 to 10 wt% were subjected to cryodesiccation and then reconstituted in DIW, which facilitated convenient use and storage. Notably, the stability of the CR@NPs remained unaffected even in the absence of cryoprotectants, such as glycerol, polyethylene glycol, or dimethyl sulfoxide, which are typically used to improve dispersion. Using methylene blue staining, we determined that the particles were well dispersed (Figure 4D (a)) and that the particles precipitated after redispersion after cryodesiccation (Figure 4D (b)).

In situ and in vitro Assessment of the Antioxidant Activity of CR@NPs

It is commonly known that CR has exceptional antioxidant abilities.[42] Achieving optimal antioxidant efficacy of CR in the aqueous phase is challenging due to its hydrophobic characteristics.[39,43] For this reason, we developed CR@NPs to enhance CR activity in water-based solutions (Figure 2B). Two methods were employed to evaluate the antioxidant potential of the CR@NPs: an in situ DPPH antioxidant activity test and an in vitro radical scavenging activity assay. A DPPH radical scavenging assay (Figure 5A) was used to evaluate the antioxidant abilities of CR@NPs compared to those of the control groups. DPPH, an organic nitrogen radical, absorbs light from the visible spectrum at a wavelength of 515 nm. When an antioxidant comes in contact with a solution containing DPPH radicals, the color of the solution changes from violet to yellow. The color change arises from the transfer of electrons or hydrogen atom from the radical scavenger to DPPH, leading to a reduction in absorbance at 515 nm. Compared to the positive control, ascorbic acid (AA) and CR in distilled water (DIW)

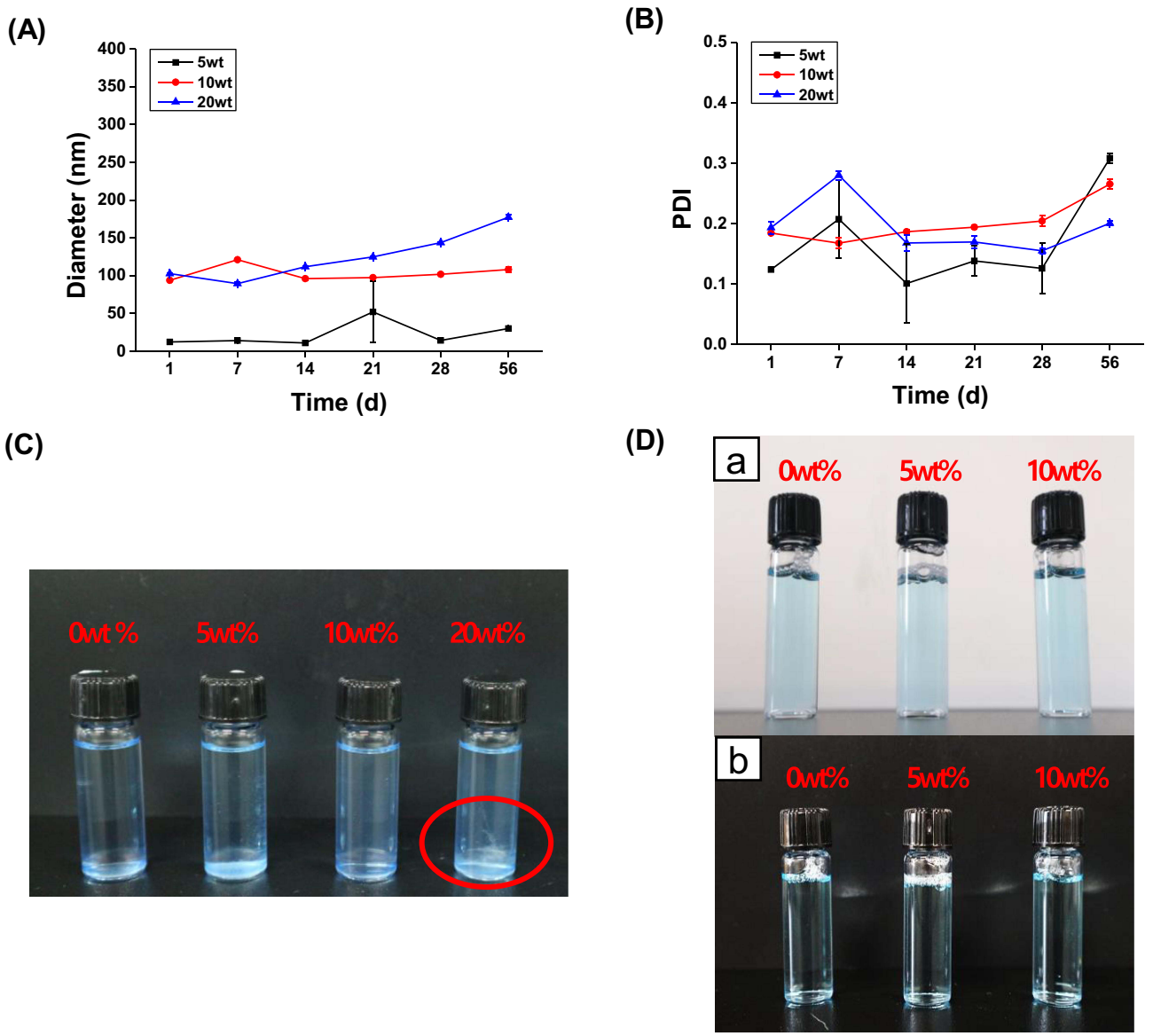

Figure 4 The long-term stability of CR@NPs with different CR loadings, ranging from 0% to 20% weight, was assessed. The following parameters were monitored over 2 months: (**A**) Changes in hydrodynamic diameters, (**B**) Polydispersity index (PDI), (**C**) Digital images of CR@NPs obtained by methylene-blue staining test taken 2 months after encapsulation. The red circle indicates the occurrence of precipitation for 20 wt% on the 56th day. (**D**) Digital image of CR@NPs with varying CR loadings (0 wt%, 5 wt%, and 10 wt%) re-dispersed in deionized water (DIW) after lyophilization for 2 days without cryoprotectants (a: to check dispersion, b: to check precipitation).

showed minimal effects on DPPH radical scavenging. This experiment demonstrated that the biological applications of *C. rotundus* are limited if they are not water-soluble unless encapsulated. However, CR@NPs showed superior DPPH radical scavenging activity compared to AA. Additionally, the antioxidant effect became more pronounced as the CR concentration in the CR@NPs increased from 5 to 10 weight percent (wt%). Moreover, in the case of 0 wt% CR@NP (which did not contain CR), only minimal scavenging of DPPH radicals was observed. This suggests that the solubilizer had little or no influence on antioxidant activity, as depicted in Figure 5A. Subsequently, H_2DCFDA, a probe for measuring ROS fluorescence, easily penetrates the cellular membrane and is rapidly oxidized to produce the highly fluorescent DCF. In the presence of intracellular ROS, DCF emits green fluorescence and its intensity at an emission wavelength of 535 nm (excitation wavelength: 485 nm) is enhanced.[44] The In vitro antioxidant activity was assessed by examining the fluorescence of H_2DCFDA after the introduction of H_2O_2 into mouse NIH 3T3 fibroblast cells (Figure 5B). H_2O_2 acts as an oxidative stressor, establishing a cellular environment that triggers ROS production. The negative control group included NIH 3T3 cells treated with H_2O_2. As

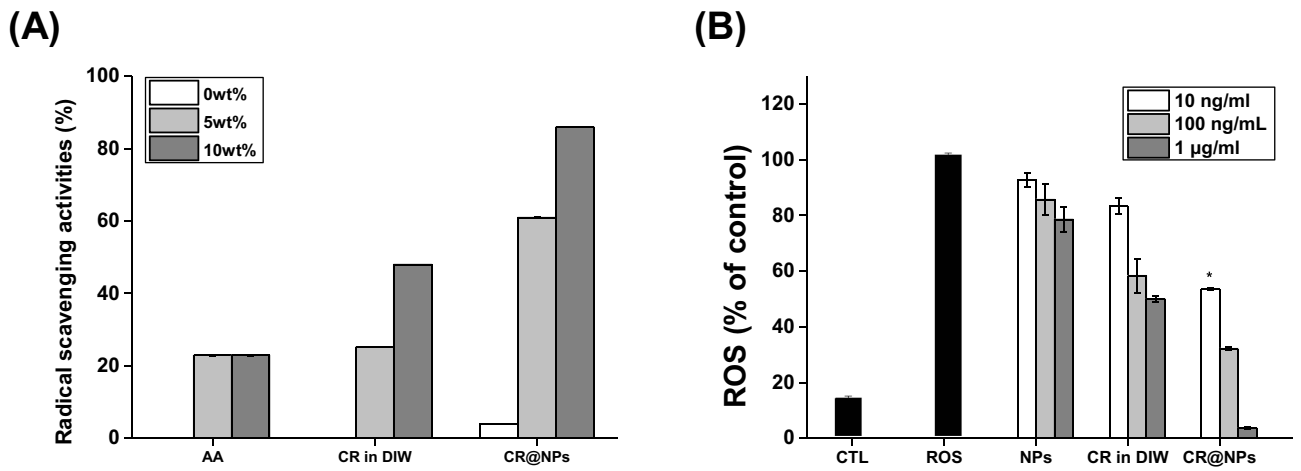

Figure 5 The antioxidant activity of CR@NPs. (**A**) The In situ assay of CR@NPs was compared to that of ascorbic acid (AA) and CR in deionized water (DIW) using the 2.2-diphenyl-1-picrylhydrazyl (DPPH) radical-scavenging assay at different concentrations (0%, 5%, and 10% by weight). (**B**) In vitro assay conducted with NIH 3T3 fibroblast cells using the H_2DCFDA assay kit. The antioxidant activity of CR@NPs 10 wt% was evaluated, in the range of 10 ng/mL to 1 μg/mL (*p < 0.05).

anticipated, cells treated with 10 wt% CR@NP exhibited a significant decrease in ROS levels, achieving approximately 50% reduction, with an increase in the CR concentration from 10 ng/mL to 1μg/mlM. Nonetheless, cells treated with 0 wt% CR@NPs and CR in DIW exhibited reduction in ROS levels by up to 78% and 50%, respectively. Consequently, we can infer that 0 wt% CR@NP had a negligible effect, and CR in distilled water (DIW) had only a limited influence on the in vitro ROS-scavenging activity, as illustrated in Figure 5B. These results highlight the enhanced antioxidant activity of encapsulated CR.

In vitro Assessment of Cytotoxicity of CR@NPs

To assess the compatibility of CR@NPs with NIH 3T3 fibroblasts, a post-treatment MTT assay was performed. The viability of NIH 3T3 cells exhibited only a slight decrease, suggesting the absence of significant toxic effects when exposed to CR at 1 to 100 μg/mL, as depicted in Figure 6A. No adverse effects were observed in NIH 3T3 cells exposed to samples at CR concentrations up to 100 μg/mL. This is supported by the fact that the cell viability remained above 90% after 24 hr. These findings indicate the biocompatibility of CR@NPs at concentrations up to 100 μg/mL without adverse effects.

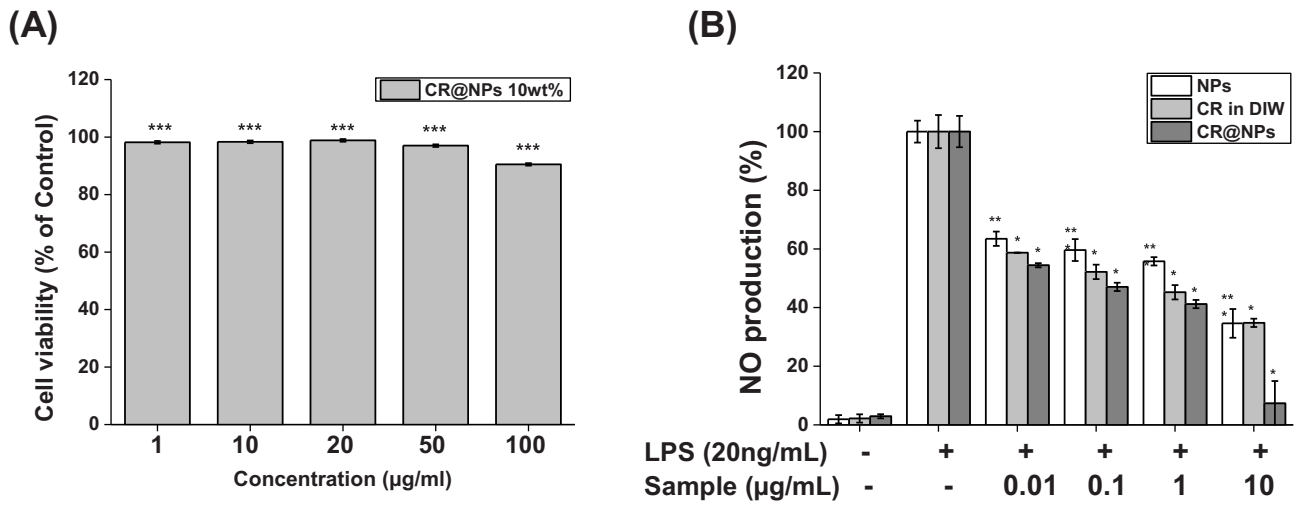

Figure 6 (**A**) Cytotoxicity analysis of CR@NPs 10wt% was performed with CR concentrations ranging from 1 to 100 μg/mL using the MTT assay kit in NIH-3T3 fibroblast cells. (**B**) Nitric oxide (NO) production analysis was conducted on CR@NPs 0wt%, 10wt%, and CR in deionized water (DIW), with concentrations ranging from 0.01 to 10 μg/mL (*p < 0.05, **p < 0.01, ***p < 0.005).

In vitro Assessment of Anti-Inflammatory Activity of CR@NPs

This study investigated the suppressive effect of CR@NPs on LPS-induced NO production in the mouse macrophage cell line RAW 264.7. NO levels were measured by analyzing the presence of NO^{2-} in the cell culture medium using Griess reagent. The study involved the simultaneous administration of different concentrations (0.01, 0.1, 1, and 10 μg/mL) of CR@NPs along with LPS (20 ng/mL), and the outcomes were compared with those of the group that received LPS alone. The Griess reaction, which uses a Griess reagent consisting of sulfanilamide and N-(1-naphthyl) ethylenediamine dihydrochloride, is a simple method to quantify NO production. In this process, a stable nitrite byproduct in the cell culture medium is converted into a purple azo dye, which can be quantified using photometric methods. Cells generate NO using different isoforms of the enzyme nitric oxide synthase (NOS), which converts L-arginine into L-citrulline and NO. When exposed to oxygen, nitric oxide (NO) breaks down into nitrite (NO^{2-}) and nitrate (NO^{3-}) (Figure 2C).[35] Treatment of RAW 264.7 cells with 10 wt% CR@NPs resulted in a significant decrease in NO levels, which was 45% lower than that of the LPS-treated group at 1 μg/mL. The concentration of α-cyperone at 1 μg/mL of CR@NP 10wt% was 0.45 nM, indicating that it has anti-inflammatory activity at very low concentrations.[7] Furthermore, at a concentration of 10 μg/mL (4.5 nM), as shown in Figure 6B, the NO level decreased by more than 93% and reached only 7.35% of the baseline value. These results confirmed that the inhibitory effect of CR@NPs on LPS-induced NO production was superior to that of unencapsulated CR in DIW even at low concentrations, demonstrating that CRHF containing α-cyperone through nanoencapsulation has sufficient anti-inflammatory properties even at low concentrations.

Conclusion

Few studies have explored the biological activities of α-cyperone, which is a primary compound in essential oils of CR rhizomes and accounts for approximately 20% of the total oil content.[45] Among the various biological activities, the anti-inflammatory properties of the essential oil of *C. rotundus* are traditionally recognized.[46] Essential oil extracted with ethanol and subsequently fractionated with n-hexane was found to inhibit NO production in LPS-induced RAW 264.7 cells more effectively than the comprehensive ethanol extract. However, a high concentration of α-cyperone is required for its anti-inflammatory effect.[7] In this study, we aimed to increase the yield of essential oils of CR using a microbubble generator to enhance the anti-inflammatory activity, and a total of 9.4% α-cyperone was obtained. Nanoparticles were prepared using nanoprecipitation to maintain the natural therapeutic activity of CR essential oils over a longer period of time and to enable easy application in an aqueous environment.[14] Using nanoprecipitation technology in combination with bio-degradable plant extracts, such as α-cyperone, and the solubilizer SJC-clearsol D to make green nanoparticles,[24] CR@NPs can be produced easily and quickly. The CR@NPs showed long-term stability and a high CRHF loading capacity. Various in situ and in vitro experiments were performed to confirm the antioxidant and anti-inflammatory properties of the CR@NPs. The optimization of these green nanomaterials is expected to advance biological and industrial applications in the pharmaceutical, food, and cosmetics industries.[47]

Abbreviations

CR, *Cyperus rotundus* L. (*C. rotundus*); CRHF, α-cyperone-rich *C. rotundus* n-hexane fraction; CR@NPs, *Cyperus rotundus*-loaded nanoparticles; DLS, dynamic light scattering; PDI, polydispersity index; HPLC, high-performance liquid chromatography; DPPH, 2.2-diphenyl-1-picrylhydrazyl; AA, ascorbic acid; CTL, control; ROS, reactive oxygen species; LPS, lipopolysaccharides; NO, nitric oxide; NOS, nitric oxide synthase; NO^{2-}, nitrite; NO^{3-}, nitrate; CO_2, carbon dioxide; DIW, deionized water; PBS, phosphate-buffered saline; DMEM, Dulbecco's modified Eagle's medium; PS, penicillin-streptomycin; FBS, fetal bovine serum; DMSO-d_6, dimethyl sulfoxide-d_6; MTT, 3-(4,5-dimethylthiazol-2-yl)-2,5-diphenyltetrazolium bromide; H_2DCFDA, 2.7-dichlorodihydrofluorescein diacetate; DCF, dichlorofluorescein.

Author Contributions

All authors have made a significant contribution to the work reported, whether in conception, study design, execution, acquisition of data, analysis, and interpretation, or in all of these areas; took part in drafting, revising, or critically reviewing the article; gave final approval for the version to be published; agreed to the journal to which the article was submitted; and agreed to be accountable for all aspects of the work.

Funding

This research was financially supported by the Ministry of Small and Medium-Sized Enterprises (SMEs) and Startups (MSS), Korea, under the "Regional Specialized Industry Development Plus Program (R&D, S3363662)" supervised by the Korea Technology and Information Promotion Agency for SMEs (TIPA). This research was supported by the Korea Institute of Marine Science and Technology Promotion funded by the Ministry of Oceans and Fisheries (RS-2023-00254302). This research was supported by the Seoul Business Agency (SBA) grant funded by the Seoul Metropolitan Government (grant number BT220140). This work was supported by the National Research Foundation of Korea (NRF) grant funded by the Korea government (MSIT) (2021M3C1C3097647).

Disclosure

Daekyung Sung, Chaehyun Kim, Juntae Bae, Jun-Hwan Jang, and Ah-Reum Jung report a patent "Method for producing Cyperus Rotundus extract nanoparticles with improved antioxidant and uses of the Cyperus Rotundus extract nanoparticles" issued. The authors report no other conflicts of interest in this work.

References

1. Oh G-S, Yoon J, Lee GG, Kwak JH, Kim S-W. The Hexane fraction of Cyperus rotundus prevents non-alcoholic fatty liver disease through the inhibition of liver X receptor α-mediated activation of sterol regulatory element binding protein-1c. *Am J Chin Med*. 2015;43(03):477–494. doi:10.1142/S0192415X15500305
2. Peerzada AM, Ali HH, Naeem M, Latif M, Bukhari AH, Tanveer A. Cyperus rotundus L.: traditional uses, phytochemistry, and pharmacological activities. *J Ethnopharmacol*. 2015;174:540–560. doi:10.1016/j.jep.2015.08.012
3. Pal D, Dutta S. Evaluation of the Antioxidant activity of the roots and Rhizomes of Cyperus rotundus L. *Indian J Pharm Sci*. 2006;68(2):256. doi:10.4103/0250-474X.25731
4. Kilani S, Ledauphin J, Bouhlel I, et al. Comparative study of Cyperus rotundus essential oil by a modified GC/MS analysis method. Evaluation of its antioxidant, cytotoxic, and apoptotic effects. *Chem Biodivers*. 2008;5(5):729–742. doi:10.1002/cbdv.200890069
5. Sun LY, Kyung HO, Woo SS, Hyun PJ. Effects of water-extracted Cyperus Rotundus on the nitric oxide production and cytokine gene expression. *J Physiol Pathol Korean Med*. 2003;17(3):771–776.
6. Lawal OA, Oyedeji AO. Chemical composition of the essential oils of Cyperus rotundus L. from South Africa. *Molecules*. 2009;14(8):2909–2917. doi:10.3390/molecules14082909
7. Jung S-H, Kim SJ, Jun B-G, et al. α-Cyperone, isolated from the rhizomes of Cyperus rotundus, inhibits LPS-induced COX-2 expression and PGE2 production through the negative regulation of NFκB signalling in RAW 264.7 cells. *J Ethnopharmacol*. 2013;147(1):208–214. doi:10.1016/j.jep.2013.02.034
8. Seo W-G, Pae H-O, Oh G-S, et al. Inhibitory effects of methanol extract of Cyperus rotundus rhizomes on nitric oxide and superoxide productions by murine macrophage cell line, RAW 264.7 cells. *J Ethnopharmacol*. 2001;76(1):59–64. doi:10.1016/S0378-8741(01)00221-5
9. Parmar R, Majumder SK. Microbubble generation and microbubble-aided transport process intensification—A state-of-The-art report. *Chem Eng Process*. 2013;64:79–97. doi:10.1016/j.cep.2012.12.002
10. Yadav G, Fabiano LA, Soh L, Zimmerman J, Sen R, Seider WD. CO2 process intensification of algae oil extraction to biodiesel. *AIChE J*. 2021;67(1):e16992. doi:10.1002/aic.16992
11. Bredwell MD, Worden RM. Mass-transfer properties of microbubbles. 1. Experimental studies. *Biotechnol Progr*. 1998;14(1):31–38. doi:10.1021/bp970133x
12. Roberto B, Fabio C, Ernesto P, et al. Essential Oils for a sustainable control of honeybee varroosis. *Veter Sci*. 2023;10(308):1–28.
13. El Asbahani A, Miladi K, Badri W, et al. Essential oils: from extraction to encapsulation. *Int J Pharm*. 2015;483(1–2):220–243. doi:10.1016/j.ijpharm.2014.12.069
14. Minost A, Delaveau J, Bolzinger M-A, Fessi H, Elaissari A. Nanoparticles via nanoprecipitation process. *Recent Pat Drug Deliv Formul*. 2012;6(3):250–258. doi:10.2174/187221112802652615
15. Oh KS, Han SK, Choi YW, Lee JH, Lee JY, Yuk SH. Hydrogen-bonded polymer gel and its application as a temperature-sensitive drug delivery system. *Biomaterials*. 2004;25(12):2393–2398. doi:10.1016/j.biomaterials.2003.09.008
16. Schettini DA, Ribeiro RR, Demicheli C, et al. Improved targeting of antimony to the bone marrow of dogs using liposomes of reduced size. *Int J Pharm*. 2006;315(1–2):140–147. doi:10.1016/j.ijpharm.2006.01.048
17. Jayaprakash N, Vijaya JJ, Kaviyarasu K, et al. Green synthesis of Ag nanoparticles using Tamarind fruit extract for the antibacterial studies. *J Photochemistr Photobiol B*. 2017;169:178–185. doi:10.1016/j.jphotobiol.2017.03.013
18. Hussain I, Singh N, Singh A, Singh H, Singh S. Green synthesis of nanoparticles and its potential application. *Biotechnol Lett*. 2016;38(4):545–560. doi:10.1007/s10529-015-2026-7
19. Baran A, Fırat Baran M, Keskin C, et al. Investigation of antimicrobial and cytotoxic properties and specification of silver nanoparticles (AgNPs) derived from Cicer arietinum L. green leaf extract. *Front Bioeng Biotechnol*. 2022;10:855136. doi:10.3389/fbioe.2022.855136
20. Suresh S, Ilakiya R, Kalaiyan G, et al. Green synthesis of copper oxide nanostructures using Cynodon dactylon and Cyperus rotundus grass extracts for antibacterial applications. *Ceram Int*. 2020;46(8):12525–12537. doi:10.1016/j.ceramint.2020.02.015
21. Omran AM. Characterization of green route synthesized zinc oxide nanoparticles using Cyperus rotundus rhizome extract: antioxidant, antibacterial, anticancer and photocatalytic potential. *J Drug Delivery Sci Technol*. 2023;79:104000. doi:10.1016/j.jddst.2022.104000
22. Rivas CJM, Tarhini M, Badri W, et al. Nanoprecipitation process: from encapsulation to drug delivery. *Int J Pharm*. 2017;532(1):66–81. doi:10.1016/j.ijpharm.2017.08.064

23. Briançon S, Fessi H, Lecomte F, Lieto J. Study of an original production process of nanoparticles by precipitation. *Récents progrès en génie des procédés*. 1999;157–164.
24. Tahara K, Sakai T, Yamamoto H, Takeuchi H, Kawashima Y. Establishing chitosan coated PLGA nanosphere platform loaded with wide variety of nucleic acid by complexation with cationic compound for gene delivery. *Int J Pharm*. 2008;354(1–2):210–216. doi:10.1016/j.ijpharm.2007.11.002
25. Devi MP, Chakrabarty S, Ghosh S, Bhowmick N. Essential oil: its economic aspect, extraction, importance, uses, hazards and quality. *Value Add Horticult Crops*. 2015;269–278.
26. Jae-seop LJ-T, Jun-hwan J, Ah-reum J, Na-ri K, Ji-yeon L, So-hyun Moon, inventor; Cosmetic composition for anti-inflammatory, skin soothing, irritation relieving and skin barrier improvement containing extract of Hyangbu-ja. South Korea patent application KR 10-2022-0170937; 2023.
27. Seo J, Kim J, Kim S, Liu T, Whang WK. Development of content analysis for Cyperus rotundus by HPLC-UV and a comparison between Chinese and domestic Cyperi Rhizoma. *Yakhak Hoeji*. 2012;56(5):280–287.
28. Kim S, Yu S, Kim J, et al. Facile Fabrication of α-Bisabolol Nanoparticles with Improved Antioxidant and Antibacterial Effects. *Antioxidants*. 2023;12(1):207. doi:10.3390/antiox12010207
29. Na Y, Lee JS, Woo J, et al. Reactive oxygen species (ROS)-responsive ferrocene-polymer-based nanoparticles for controlled release of drugs. *J Mat Chem B*. 2020;8(9):1906–1913. doi:10.1039/C9TB02533B
30. Yu S, Kim S, Kim J, et al. Highly Water-Dispersed and Stable Deinoxanthin Nanocapsule for Effective Antioxidant and Anti-Inflammatory Activity. *Int j Nanomed*. 2023;Volume 18:4555–4565. doi:10.2147/IJN.S401808
31. Yang H, Yu S, Kim J, et al. Facile Solvent-Free Preparation of Antioxidant Idebenone-Loaded Nanoparticles for Efficient Wound Healing. *Pharmaceutics*. 2022;14(3):521. doi:10.3390/pharmaceutics14030521
32. Apak R, Gorinstein S, Böhm V, Schaich KM, Özyürek M, Güçlü K. Methods of measurement and evaluation of natural antioxidant capacity/activity (IUPAC Technical Report). *Pure Appl Chem*. 2013;85(5):957–998. doi:10.1351/PAC-REP-12-07-15
33. Oh H, Lee JS, Sung D, Lim J-M, Choi WI. Potential antioxidant and wound healing effect of nano-liposol with high loading amount of astaxanthin. *Int j Nanomed*. 2020;Volume 15:9231–9240. doi:10.2147/IJN.S272650
34. Xu L, Zhao M, Gao W, et al. Polymeric nanoparticles responsive to intracellular ROS for anticancer drug delivery. *Colloids Surf B*. 2019;181:252–260. doi:10.1016/j.colsurfb.2019.05.064
35. Dirsch VM, Stuppner H, Vollmar AM. The Griess assay: suitable for a bio-guided fractionation of anti-inflammatory plant extracts? *Planta med*. 1998;64(05):423–426. doi:10.1055/s-2006-957473
36. Marrone BL, Lacey RE, Anderson DB, et al. Review of the harvesting and extraction program within the National Alliance for Advanced Biofuels and Bioproducts. *Algal Res*. 2018;33:470–485. doi:10.1016/j.algal.2017.07.015
37. Fujikawa S, Zhang R, Hayama S, Peng G. The control of micro-air-bubble generation by a rotational porous plate. *Int J Multiphase Flow*. 2003;29(8):1221–1236. doi:10.1016/S0301-9322(03)00106-X
38. Tsuge H. Fundamentals of microbubbles and nanobubbles. *Bull Soc Sea Water Sci Japan*. 2010;64(1):4–10.
39. Nafisah W, Pinanti H, Christina Y, Soewondo A, Rifa'i M, Djati M. *Potency of Cyperus Rotundus Bioactive Compound Against Anti-Apoptotic Protein: An in silico Approach*. IOP Publishing; 2021:012067.
40. Gupta M, Palit T, Singh N, Bhargava K. Pharmacological studies to isolate the active constituents from Cyperus rotundus possessing anti-inflammatory, anti-pyretic and analgesic activities. *Indian J Med Res*. 1971;59(1):76–82.
41. Azimi A, Ghaffari SM, Riazi GH, Arab SS, Tavakol MM, Pooyan S. α-Cyperone of Cyperus rotundus is an effective candidate for reduction of inflammation by destabilization of microtubule fibers in brain. *J Ethnopharmacol*. 2016;194:219–227. doi:10.1016/j.jep.2016.06.058
42. Nagulendran K, Velavan S, Mahesh R, Begum VH. In vitro antioxidant activity and total polyphenolic content of Cyperus rotundus rhizomes. *J Chem*. 2007;4:440–449.
43. Sonwa MM, König WA. Chemical study of the essential oil of Cyperus rotundus. *Phytochemistry*. 2001;58(5):799–810. doi:10.1016/S0031-9422(01)00301-6
44. Choi S-I, Lee JS, Lee S, et al. Antioxidant and anti-aging effects of extracts from leaves of Castanea crenata Siebold & Zucc. in human dermal fibroblast. *J Food Hyg Saf*. 2017;32(3):243–248. doi:10.13103/JFHS.2017.32.3.243
45. Kilani S, Sghaier MB, Limem I, et al. In vitro evaluation of antibacterial, antioxidant, cytotoxic and apoptotic activities of the tubers infusion and extracts of Cyperus rotundus. *Bioresour Technol*. 2008;99(18):9004–9008. doi:10.1016/j.biortech.2008.04.066
46. Dang G, Parekar R, Kamat S, Scindia A, Rege N. Antiinflammatory activity of Phyllanthus emblica, Plumbago zeylanica and Cyperus rotundus in acute models of inflammation. *Phytother Res*. 2011;25(6):904–908. doi:10.1002/ptr.3345
47. Nicolas J, Mura S, Brambilla D, Mackiewicz N, Couvreur P, Design FS. Biomedical applications of targeted biodegradable/biocompatible polymer-based nanocarriers for drug delivery. *Chem Soc Rev*. 2013;42(3):1147–1235. doi:10.1039/c2cs35265f